DAMAGE VARIATIONS ON LOW-CRESTED BREAKWATERS

Rolando Garcia [1] and Nobuhisa Kobayashi [2]

The cross-shore numerical model CSHORE extended to oblique waves is used to predict the spatial variation of damage on different sections of the trunk and head of a low-crested breakwater. The agreement is mostly within a factor of 2 but the model overpredicts damage on the back head of a submerged structure. An experiment was conducted in a wave flume for a low-crested stone structure located inside the surf zone on a sand beach. The model is shown to reproduce the measured cross-shore wave transformation on the beach without and with the structure as well as the measured small damage on the structure.

Keywords: low-crested breakwater; rubble mound; damage; trunk; head

INTRODUCTION

Low-crested stone structures (LCS) are constructed to provide sheltered areas with some wave transmission. Damage on LCS depends on its crest height above the still water level (SWL) and varies spatially on the trunk and head of the breakwater. The cross-shore numerical model CSHORE was developed to predict irregular wave breaking and transmission over and through a submerged porous structure (Kobayashi, et al., 2007) and was extended to predict damage progression on a conventional stone breakwater with little wave overtopping (Kobayashi, et al., 2010) and deformation of a reef breakwater with wave transmission (Kobayashi, et al., 2013).

In this study, CSHORE is extended to obliquely incident waves and compared with available data on wave transmission and damage on different trunk and head sections of a LCS. Comparisons of wave transmission prediction against available data for obliquely incident waves are presented in Garcia and Kobayashi (2014). The damage on the front and back sections of the round head is predicted assuming similarity of head and trunk damage for LCS. An experiment was conducted for a LCS located inside the surf zone on a sand beach during a storm in order to assess the utility of CSHORE for a typical field application.

NUMERICAL MODEL

Figure 1 depicts a LCS with its crest below the SWL. The cross-shore coordinate x is positive onshore with $x = 0$ at the seaward location of the incident irregular wave measurement. The irregular waves are represented by the spectral significant wave height H_{m0} and spectral peak period T_p. CSHORE assumes alongshore uniformity with the alongshore coordinate y parallel to the straight trunk. The vertical coordinate z is positive upwards with $z = 0$ at the SWL. The upper and lower boundaries of the breakwater are located at $z = z_b$ and z_p, respectively, where the lower boundary is assumed to be fixed and impermeable.

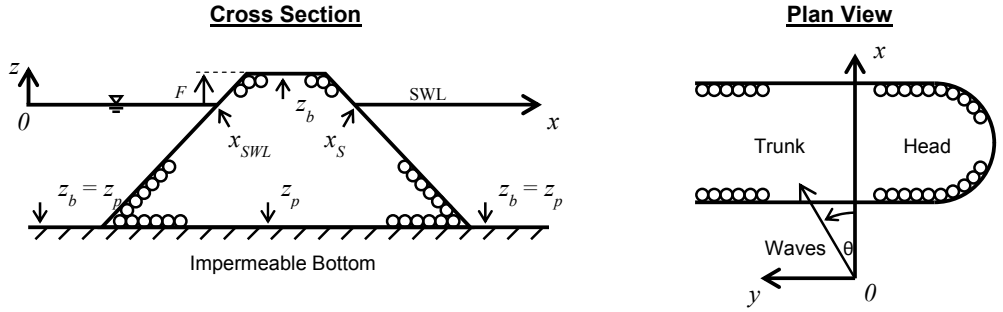

Figure 1. Onshore (*x*), alongshore (*y*), and vertical (*z*) coordinates of numerical model.

[1] PRDW-AV Consulting Port and Coastal Engineers, Chile, rgarcia@prdw.com, rgarcia@udel.edu
[2] Center for Applied Coastal Research, University of Delaware, nk@udel.edu

For the seaward wet zone of $x < x_{SWL}$ and the entire zone above the submerged structure, the time-averaged continuity, cross-shore momentum, longshore momentum and energy equations along with Snell's law are used to compute the cross-shore variations of the wave angle θ and the mean and standard deviation of the free surface elevation η above the SWL and the depth-averaged cross-shore velocity U and longshore velocity V above the permeable bottom. The time-averaged cross-shore water flux and wave energy dissipation inside the porous structure are included by extending the approximate porous flow model for $\theta = 0$ (Kobayashi, et al., 2007) to oblique waves as presented in the report of Kobayashi (2013). The longshore water flux inside the porous structure is neglected assuming the negligible longshore momentum flux into and out of the porous structure.

For the intermittently wet and dry zone of $x_{SWL} < x < x_S$ the wave angle θ is assumed to remain the same as the computed angle θ at $x = x_{SWL}$. The cross-shore variations of the mean and standard deviation of η, U and V are computed using the probabilistic model of Kobayashi, et al. (2010) coupled with the time-averaged nonlinear shallow-water wave equations with the assumption of $(\sin \theta_{SWL})^2$ being much smaller than unity (Farhadzadeh, et al., 2012). The vertical water and cross-shore momentum fluxes into the porous structure are included in the time-averaged continuity and cross-shore momentum equations. In the landward wet zone of $x > x_s$, the simple linear wave model including the water flux inside the porous structure (Kobayashi, 2013) is used to compute the cross-shore variations of the mean and standard deviation of η and U, where the mean and standard deviation of V are assumed to be negligible.

After computation of the cross-shore hydrodynamics, CSHORE computes the time-averaged cross-shore and longshore transport rates using the bed load formula of Kobayashi, et al. (2009) with the criterion for initiation of stone movement proposed by Kobayashi, et al. (2010). The temporal change of the bottom elevation $z_b(x,t)$ is computed using the conservation equation of stone volume per unit alongshore width. The erosion depth is then calculated as $d_e(x,t) = [z_b(x,0) - z_b(x,t)] > 0$. By integrating the erosion depth along a specified trunk section, the eroded area A_e is obtained and the damage S_p is computed with Equation (1).

$$S_p = \frac{A_e}{D_{n50}^{\ 2}} \tag{1}$$

where

S_p : damage based on the measured profile
A_e : eroded area on the cross-shore section.
D_{n50} : nominal stone diameter = $(M_{50}/\rho_s)^{1/3}$
M_{50} : medium mass of the stone
ρ_s : density of the stone

AVAILABLE EXPERIMENTAL DATA

Use is made of the wave basin experiments at National Research Council of Canada (NRC) by Vidal & Mansard (1995a) and Aalborg University, Denmark (AAU) by Kramer & Burcharth (2003) as listed in Table 1. In NRC and AAU experiments, damage was measured on different sections over the total section (TS) of the trunk as shown schematically on Figure 2. In NRC experiment FS = front slope, C = crest and BS = back slope, where the C section overlapped with FS and BS sections. In AAU experiment SS = seaward slope, C = crest and LS = leeward slope. Head damage was measured on the front head section FH and back head section BH in NRC experiments which are equivalent to seaward head section SH and middle head plus leeward head section (MH+LH) in AAU experiments, respectively. In NRC experiments, a steel frame and a wire mesh were used to partially cover the breakwater, exposing the specific sections to be analyzed. In AAU experiments colored stones were used to identify sections on the trunk and round head.

Table 1: Tests conditions of available experimental data.

Data	NRC	AAU
Number of tests	35	69
Test duration (min)	60	14 to 136
Structure height (cm)	40, 60	30
Crest width (cm)	15	10, 25
Seaward slope	1/1.5	1/2
Landward slope	1/1.5	1/2
Freeboard F (cm)	–5 to 6	–10 to 5
Armor stone D_{n50} (cm)	2.5	3.3
Core stone D_{n50} (cm)	1.9	1.4
Wave angle θ (degrees)	0	–21 to 26
Wave height H_{m0} (cm)	5 to 15	4 to 25
Wave period T_p (s)	1.4 to 1.8	0.9 to 2.5

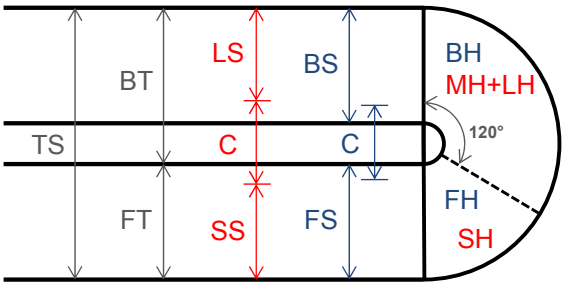

Figure 2: Definition of breakwater trunk and head sections. NRC sections (blue), AAU sections (red).

In NRC experiment, damage on each trunk section was measured in two ways: by measuring the eroded area of the cross-shore profile change (damage S_p) and by counting the number of stones displaced at least D_{n50} (damage S_v), as shown by Equation (2). On head sections and in AAU experiment, the profile change was not measured and only damage S_v is available.

$$S_v = \frac{N_y \, D_{n50}}{(1-n_p)\, l_y} \qquad (2)$$

where
S_v : damage based on the number of displaced stones
D_{n50} : nominal stone diameter
N_y : number of displaced stones over the alongshore length l_y
n_p : porosity of the armor layer
l_y : alongshore length of the armor layer

If the volume of the displaced stones is equal to the eroded stone volume, then damage S_v and S_p are equal. Nevertheless, dislodged stones can fall into the void left by other displaced stones. Hence, damage S_v is expected to be larger than damage S_p.

Relation between damage S_v and S_p was examined using trunk damage measurements of NRC tests, where 6 tests exceeded destruction damage criterion (removal of core stone) given by Vidal, et al. (1992). These 6 tests were excluded in the following. Figure 3 shows S_v vs S_p for trunk sections TS, FS, C and BS. Damage S_v turns out to be larger than S_p and a linear regression analysis yields:

$$S_v = 1.24\, S_p \qquad (2)$$

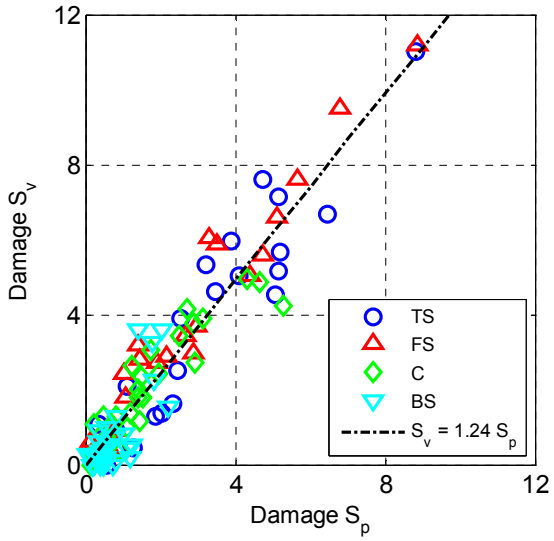

Figure 3: Measured damage S_v versus S_p for trunk sections in NRC data.

In the subsequent comparisons of the measured and computed S_v, the computed damage S_p is converted to S_v using Equation (3) for the NRC structure with 1/1.5 slope, because the numerical model cannot predict the number of displaced stones. However, the accuracy of Equation (3) is uncertain for the AAU structure with 1/2 slope.

DAMAGE ON TRUNK

The numerical model is compared with the measured damage data by Vidal and Mansard (1995a) for which a wire mesh was used to expose the designated sections showed in Figure 2. CSHORE provides two options to account for the wire mesh effect on stone movement. The first option assumes no effect on stone movement under the mesh and erosion and deposition is allowed everywhere. The second option assumes fixed stones under the mesh and erosion is allowed only over exposed sections while deposition is allowed everywhere. The computed damage is similar for the two options except for the back slope damage which is underpredicted for the second option, which suggests that the back slope damage may have been influenced by the stone movement under the mesh seaward of the back slope. The following computed results are based on the first option which neglects the wire mesh.

Figure 4 shows computed damage against measured damage in NRC experiments for the designated trunk sections TS, FS, C and BS. A linear regression is indicated in red. Damage on TS and FS sections is predicted within a factor of two for almost all tests. Damage on C section is overpredicted. Damage on BS section is predicted with less accuracy as expected for lower damage values.

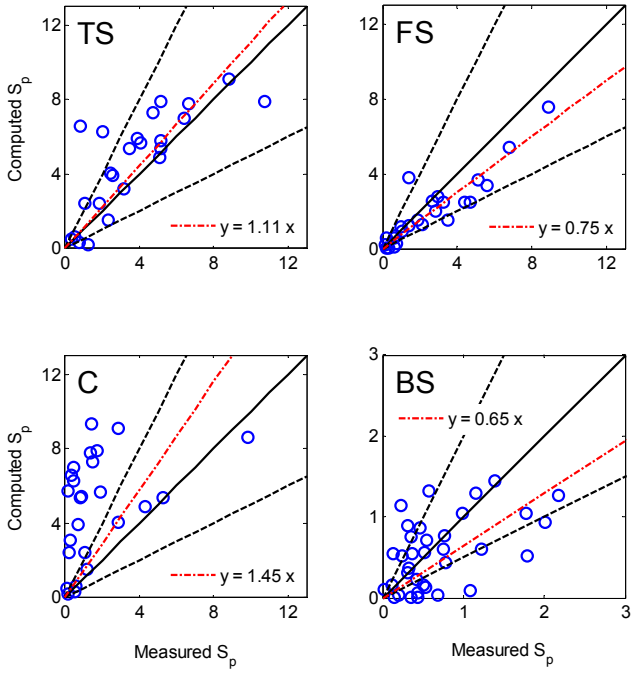

Figure 4: Damage comparison on trunk sections in NRC data.

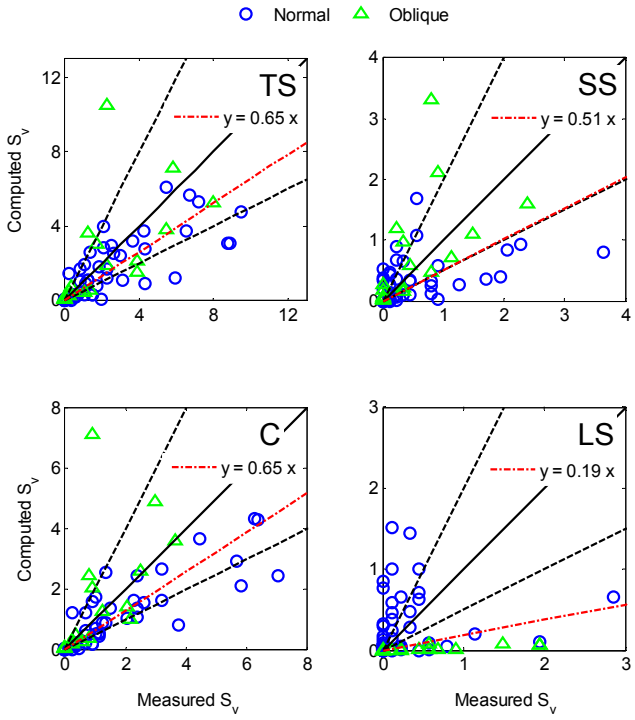

Figure 5: Damage comparison on trunk sections in AAU data.

Comparison with measured damage data by Kramer & Burcharth (2003) is shown in Figure 5 for the designated trunk sections TS, SS, C and LS as presented in Figure 2, for normal and obliquely incident waves, where oblique waves are limited to emerged structures with freeboard F = 5 cm. A linear regression is also shown. Damage on TS and C trunk sections are predicted mostly within a factor of two. Damage prediction for SS section shows more scatter in comparison to FS section in NRC data. The small measured damage on LS section is predicted poorly. Overall, the degree of agreement in Figure 5 is not as good as in Figure 4, possibly because Equation (3) based on the NRC structure with the seaward and landward slopes of 1/1.5 may not be accurate for the AAU structure with the 1/2 slope.

DAMAGE ON HEAD

In NRC experiment, the number of displaced stones on FH and BH sections exposed to unidirectional random waves with wave angle θ = 0 was measured and the corresponding damage S_v was calculated using Equation (2) where the alongshore length l_y was replaced by a representative arc length of a head section as explained by Vidal et al. (1995b). In the AAU experiment, the round head was separated into the seaward head (SH), middle head (MH) and leeward head (LH), each with an arc angle of 60°. FH and SH sections are the same, while BH section in NRC experiment corresponds to the sum of MH and LH sections in AAU experiment, as depicted in Figure 2.

Similarity of trunk and head damage for a low-crested breakwater was examined for head damage prediction with CSHORE. Measured damage on head sections was compared to that of different trunk sections. Hereby, damage on FH and BH sections on the head are assumed to be similar to the front trunk section (FT) and the back trunk section (BT), respectively, where FT and BT sections are indicated in Figure 2. The damage similarity between FH and FT sections was apparent in the NRC damage data (Vidal et al. 1995b) where FS section is the same as FT section in Figure 2. The damage similarity between BH and BT sections cannot be assessed using the NRC and AAU data directly because damage on BT section was not measured specifically.

Figure 6 shows computed head damage against measured damage in NRC experiments. Damage on FH section is predicted mostly within a factor of two. Damage prediction on BH section shows similar agreement, except for submerged structures for which damage is overpredicted by the use of this similarity assumption. The back head section is more sensitive to freeboard effects than trunk sections, as reported by Vidal, et al. (1995b).

Figure 7 shows computed head damage against measured damage in AAU experiments. The oblique wave data are limited to emerged structures with F = 5 cm. The agreement for SH section is not as good as for FH section in NRC experiment. For (MH+LH) section, damage is overpredicted for submerged structures and underpredicted for emerged structures.

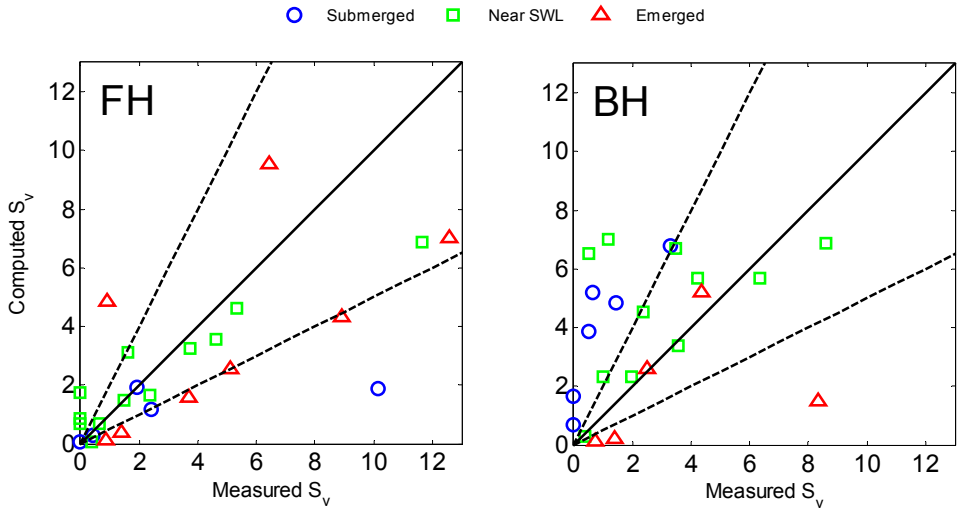

Figure 6: Measured and computed damage S_v for head sections FH and BH in NRC experiment.

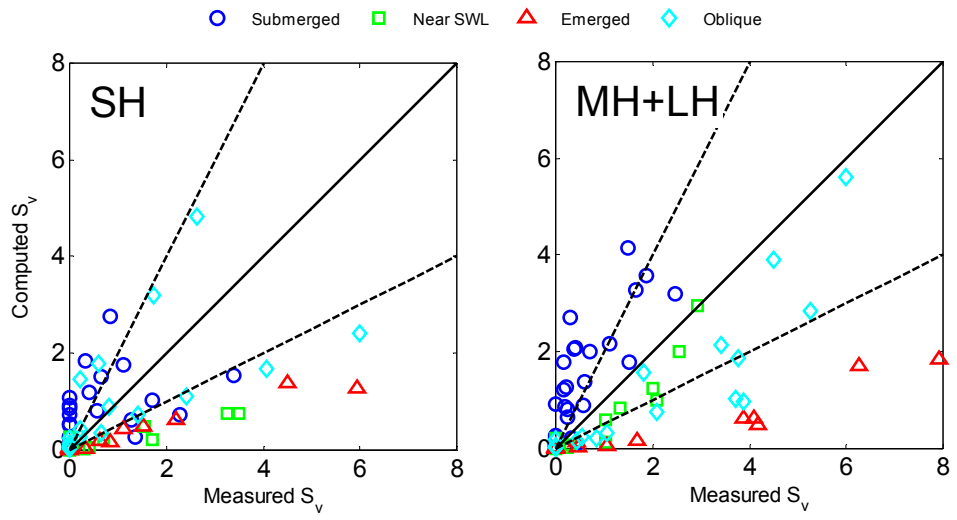

Figure 7: Measured and computed damage S_v for head sections SH and (MH+LH) in AAU experiment.

EXPERIMENT

The NRC and AAU experiments were conducted over fixed bottom and in the outer surf zone. Low-crested structures (LCS) are typically located on a sandy beach and inside the surf zone during storm conditions. Sumer et al. (2005) investigated local scour around low-crested structures located outside the surf zone on sand bottoms. An experiment was conducted in the wave flume of the Center for Applied Coastal Research of the University of Delaware, to analyze damage on a LCS and sand transport in the vicinity of the structure for typical field applications in presence of wave setup and undertow current.

The wave flume was 30 m long, 2.5 m wide and 1.5 m high. The experiment was carried out in a 23 m long and 1.15 m wide section of the wave flume as shown in Figure 8. The bottom consisted of sand on a plywood bottom slope. A partition wall in the middle reduced the amount of sand used for the beach and seiching development in the wave flume.

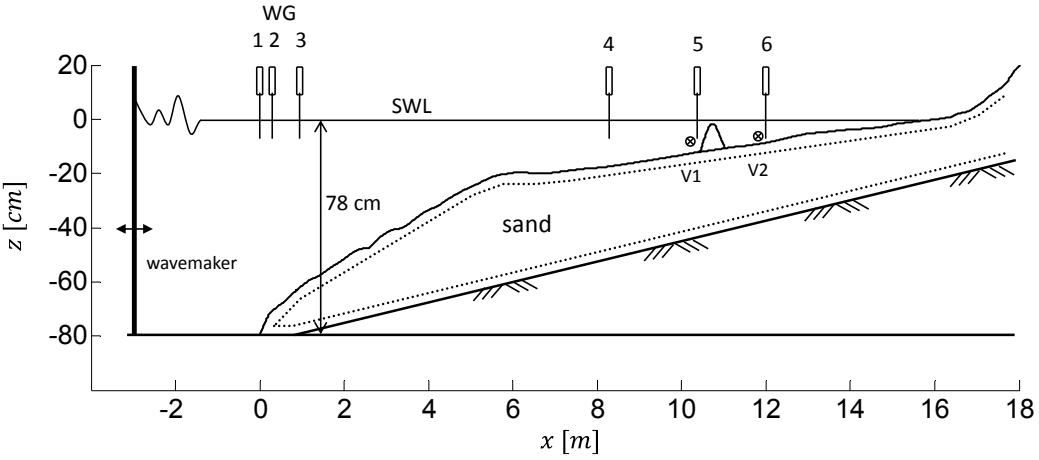

Figure 8: Experimental setup.

Six wave gauges were used to measure the free surface elevation η above SWL. Wave gauge (WG) 1 was located 3 m landward of the wave paddle. WG 1-3 were used to separate incident and

reflected waves. WG 4 was located in the outer surf zone. WG 5 and 6 were located at the toe and 1 m landward of a submerged stone structure, respectively. Fluid velocities at the cross-shore locations of WG 5 and 6 were measured using two acoustic velocimeters (V1 and V2) at an elevation of 2/3 of the local water depth below SWL. A laser line scanner mounted on a motorized cart was used to measure the sand and stone bottom elevation after lowering the water level. An array of three submerged ultrasonic transducers was used to measure the beach profile in the zone of $x = 0 – 5$ m. The measured three-dimensional profiles were averaged alongshore to obtain the cross-shore profile $z_b(x)$. Digital video and photos were used to identify displaced stones.

The median diameter, fall velocity, density, and porosity of the well sorted sand in the flume were 0.18 mm, 2.0 cm/s, 2.6 g/cm^3, and 0.4, respectively. Green (G), blue (B) and white (W) stones were used to build the breakwater. G and B stones were used as armor layers to examine their damage initiation and W stones were used to build a small core. The measured stone characteristics are summarized in Table 2.

Table 2: Measured stone characteristics

Parameter		G (green)	B (blue)	W (white)
ρ_s	[g/cm^3]	2.94	3.06	2.72
n_p		0.44	0.44	0.43
D_{n50} (50% finer)	[cm]	3.52	3.81	1.80

Two test series were conducted: with no structure (N) and with structure (S). Each series consisted of 10 runs of a 400 s burst of irregular waves generated by a piston-type wave paddle. The initial transition of 20 s was removed for the subsequent analysis of data sampled at a rate of 20 Hz. Water depth at the paddle was kept at 78 cm in the experiment. The spectral peak period T_p was 1.7 s. The spectral significant wave height H_{m0} was approximately 17 cm.

The first N test was intended to examine the cross-shore wave transformation without a structure and the degree of the beach profile change. The beach was exposed to the same wave conditions in a preliminary test and regarded to be quasi equilibrium. The beach profile was measured at the beginning of N test and after 5 and 10 runs. The measured profile changes were less than 1 cm and related to the movement of ripples whose heights and lengths were about 1 and 10 cm, respectively.

Before S test, the stone structure was constructed on the beach whose profile was measured after N test. The height of the structure was approximately 10 cm above the local bottom whose slope was 1/50. The freeboard F of the submerged structure was approximately -2 cm. The seaward and landward slopes of the structure were 1/2. The stones were placed on polyester fabric mesh with an opening of 0.074 mm that was laid on the well-sorted sand of 0.18 mm. Toe protection is normally required against scour (Burcharth et al. 2006) but was not provided in S test to examine the interaction of the armor stone and sand. The profile of the constructed structure was measured using the laser line scanner. The repeated measurements indicated that the elevation uncertainty or error was about 2 mm on the stone surface in comparison to 1 mm on the sand surface reported by Figlus et al. (2011).

The numerical model is shown to reproduce the measured cross-shore wave transformation on the beach without and with the structure. Comparison of the computed and measured hydrodynamics is shown in Garcia and Kobayashi (2014).

The numbers of displaced G and B stones were counted after each 400 s run to obtain the temporal variation of damage S_v using Equation (2) with the alongshore length $l_y = 62$ and 53 cm for G and B stones, respectively. The measured damage S_v was less than 0.5 after ten 400 s runs. The beach and structure profiles were measured after 5 and 10 runs. The measured profiles at time $t = 2{,}000$ and 4,000 s were compared with the initial profile at $t = 0$. The beach profile changed mostly before $t = 2{,}000$ s and the structure profile change of about 2 mm could not be measured reliably. The measured profiles and eroded depth in the vicinity of the structure at $t = 0$ and 4,000 s are shown in Figure 9. Sand erosion and accretion occurred seaward and landward of the structure, respectively, probably because the structure interrupted the offshore sediment transport caused by the undertow current. The eroded depth d_e (positive) of sand seaward of the structure was about 1 cm, while accretion (negative) landward of the structure was about 0.5 cm.

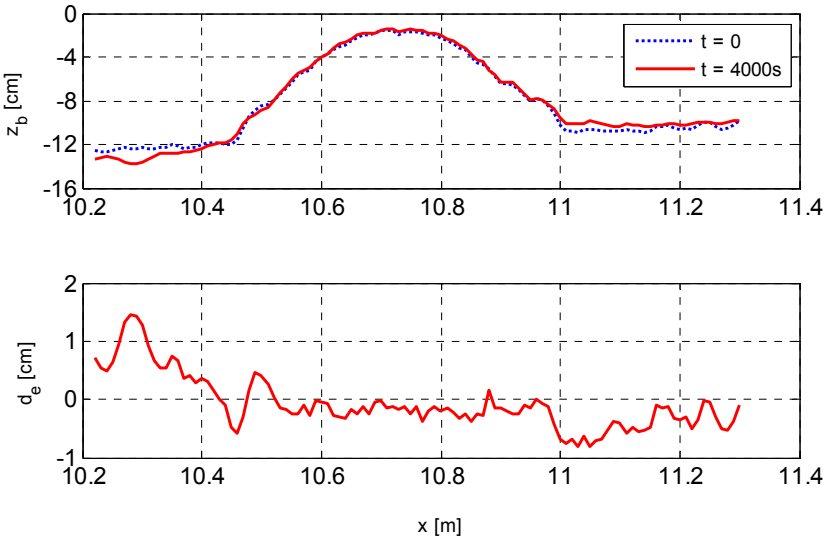

Figure 9: Measured profiles near the structure at the beginning and end of S test.

The number of displaced green (G) and blue (B) stones was determined after each run using digital photographs taken from a fixed location in front of the structure and the fine resolution laser scan. Figure 10 show pictures and Figure 11 analyzed data from the fine resolution laser scan at the beginning (S 00) and after ten runs (S 10) in the S test series. Stones located at the front toe of the structure were displaced. Only one stone moved more than the nominal stone diameter D_{n50} from its original position. Five stones moved more than 0.5 D_{n50} and are included in the calculated damage S_v using Equation (2).

Figure 10: Picture of the structure at the beginning (S 00) and after ten runs (S 10).

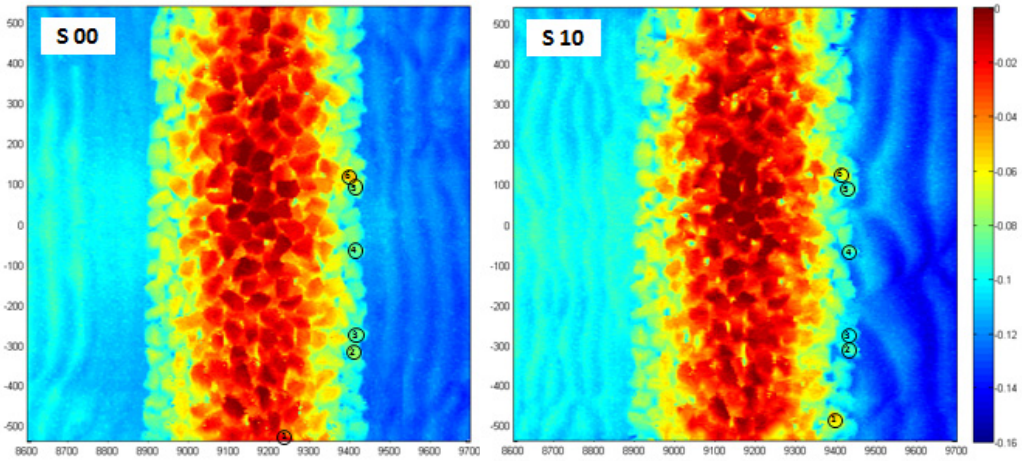

Figure 11: Fine resolution laser scan of the structure at the beginning (S 00) and after ten runs (S 10).

Measured and computed temporal variations of damage S_v for G and B stones are shown in Figure 12. The computed temporal variation is smooth because the numerical model does not predict the displacement of individual stones. The numerical model underpredicts the damage, partly because the measured damage includes three G stones and two B stones that were placed on the edge of the fabric mesh at the toe of the structure and displaced seaward over a distance of 2 to 3 cm (more than 0.5 D_{n50} but less than D_{n50}) because of no toe protection. If these displaced stones are excluded, the measured values of damage S_v would be 0.1 and 0.0 for G and B stones, respectively.

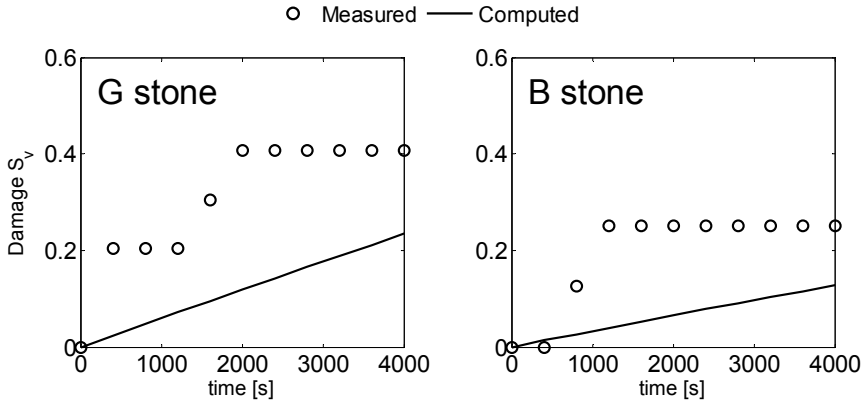

Figure 12: Measured and computed temporal variations of damage S_v in the experiment.

CONCLUSIONS

The cross-shore numerical model CSHORE developed for normally-incident irregular waves on a porous structure is extended to oblique waves in order to predict oblique wave transmission landward of a low-crested stone structure. The model is used to predict the spatial variation of damage on the trunk of the low-crested stone structure. The comparison with two data sets consisting of 104 tests indicates that the model can predict damage on the front slope, back slope, and total section mostly within a factor of 2 except for small damage on the back slopes. Similarity of trunk and head damage for a low-crested stone structure is proposed to predict damage on front head and back head sections using the cross-shore model developed for the trunk sections. The agreement for the head sections is not as good as that for the trunk sections and the model overpredicts damage on the back head of a submerged structure. The extended model may be used to predict damage progression during a severe

storm with time-varying waves and water level conditions. Such a prediction is required for the design of a low-crested structure because of its sensitivity to both waves and water level. A site-specific laboratory experiment is recommended to calibrate the model and improve the accuracy of its prediction.

An experiment was conducted in a wave flume for a low-crested stone structure located inside the surf zone on a sand beach for typical field applications. The measured small damage on the structure was difficult to predict accurately. The measured beach profile change and deposited sand height inside the porous structure (Garcia and Kobayashi 2014) indicate that the interaction of sand and stone is important in predicting local scour and deposition in the vicinity of the porous structure. This interaction is not included in the present numerical model.

ACKNOWLEDGEMENTS

The first author was supported by Fulbright Chile Program and Conicyt during his two-year Master's study at the University of Delaware.

This study was partially supported by the Artificial Reef Research Center for High Wave Control, Kwandong University in Korea and by the U.S. Army Corps of Engineers under Contract No. W911XK-13-P-0065. The writers would like to thank César Vidal for providing his report.

REFERENCES

Burcharth, H., Kramer, M., Lamberti, A. and Zanuttigh, B., (2006). Structural stability of detached low crested breakwaters. *Coastal Engineering*, 53(4), pp. 381-394.

Farhadzadeh, A., Kobayashi, N. and Gravens, M., (2012). Effect of breaking waves and external current on longshore sediment transport. *Journal of Waterway, Port, Coastal, and Ocean Engineering*, 138(3), pp. 256-260.

Figlus, J., Kobayashi, N., Gralher, C. and Iranzo, V., (2011). Wave overtopping and overwash of dunes. *Journal of Waterway, Port, Coastal, and Ocean Engineering*, 137(1), pp. 26-33.

Garcia, R. and Kobayashi, N., (2014). Trunk and head damage on a low-crested breakwater. *Journal of Waterway, Port, Coastal, and Ocean Engineering*, (in press).

Kobayashi, N., (2013). Cross-shore numerical model CSHORE 2013 for sand beaches and coastal structures. Research Report. No CACR-13-01, Center for Applied Coastal Research, University of Delaware.

Kobayashi, N., Buck, M., Payo, A. and Johnson, B., (2009). Berm and dune erosion during a storm. *Journal of Waterway, Port, Coastal, and Ocean Engineering*, 135(1), pp. 1-10.

Kobayashi, N., Farhadzadeh, A. and Melby, J., (2010). Wave overtopping and damage progression of stone armor layer. *Journal of Waterway, Port, Coastal, and Ocean Engineering*, 136(5), pp. 257-265.

Kobayashi, N., Meigs, L., Ota, T. and Melby, J., (2007). Irregular breaking wave transmission over submerged porous breakwater. *Journal of Waterway, Port, Coastal, and Ocean Engineering*, 133(2), pp. 104-116.

Kobayashi, N., Pietropaolo, J. and Melby, J., (2013). Deformation of reef breakwaters and wave transmission. *Journal of Waterway, Port, Coastal, and Ocean Engineering*, 139(4), pp. 336-340.

Kramer, M. and Burcharth, H., (2003). Wave basin experiment final form, 3-D stability tests at AAU. Report of DELOS EVK-CT-2000-0004 (www.delos.unibo.it).

Sumer, B. et al., (2005). Local scour at roundhead and along the trunk of low crested structures. *Coastal Engineering*, 52(10-11), pp. 995-1025.

Vidal, C., Losada, M. and Mansard, E., (1995b). Stability of low-crested rubble-mound breakwater heads. *Journal of Waterway, Port, Coastal, and Ocean Engineering*, 121(2), pp. 114-122.

Vidal, C., Losada, M., Medina, R. and Mansard, E., (1992). A universal analysis for the stability of both low-crested and submerged breakwaters. *Proceedings of 23rd International Conference on Coastal Engineering*, Issue 23, pp. 1679-1692.

Vidal, C. and Mansard, E., (1995a). On the stability of reef breakwaters. Technical Report. National Research Council of Canada, Otawa, Canada.